Development of a Non-contact Modular Screening Center (NCMSC) for COVID-19

Jinkyun Cho [a], *Jinho* Kim [b], *Jongwoon* Song [c], *Seungmin* Jang [a]

[a] Department of Building and Plant Engineering, Hanbat National University, Daejeon, Republic of Korea, jinkyun.cho@hanbat.ac.kr

[b] Department of Fire Protection, Safety and Facilities, Suwon Science College, Hwasung , Republic of Korea, jinho.kim@ssc.ac.kr

[c] E-SOLTEC Co., Ltd, Gwangju, Korea, kb9503@hanmail.net

Abstract. Under the global landscape of the prolonged COVID-19 pandemic, the number of individuals who need to be tested for COVID-19 through screening centers is increasing. However, there is a risk of cross-infection at each stage of the screening process. To address the risk of cross-infection in the screening center during the COVID-19 testing process, a non-contact modular screening center (NCMSC) was developed that uses biosafety cabinets and negative pressure booths to improve the problems of existing screening centers and enable safe, fast, and convenient COVID-19 testing. The main purpose of this study is to evaluate the effect of the cross-infection prevention of viruses and ventilation performance for rapid virus removal from the indoor space using both numerical analysis and experimental measurements. Computational fluid dynamics (CFD) simulations were used to determine the ventilation rate and pressure difference. We also characterized the airflow dynamics of NCMSCs using the particle image velocimetry (PIV). Moreover, design optimization was performed with three alternatives based on the air change rates and the balance of supply air (SA)/exhaust air (EA) as a ventilation strategy for preventing viral transmission.

1. Introduction

In the past, most types of viruses that reached the pandemic level were respiratory infections such as influenza and coronavirus [1]. As shown in **Fig. 1**, influenza viruses mutate continuously and the antigenic shift occurs every 40 to 50 years, leading to a pandemic situation. Particularly, the coronavirus causes a pandemic every 5 to 10 years [2]. The WHO (word health organization) declared COVID-19 a global pandemic in 2020, which persists at the present. There is a possibility that the COVID-19 outbreak started from a hospital and transmitted to the community because HCWs (health care workers) are positioned at the interface between the medical environment and local community [3], [4]. Therefore, medical institutions isolate symptomatic patients from general patients through screening centers. The screening center plays a primary role in screening suspected patients of COVID-19. According to the Ministry of Health and Welfare of Korea, as of August 2021, more than 600 screening centers have been installed and are under operation in Korea. Temporary, drive-through and walk-through screening centers have been installed

as top-priority countermeasures to overcome the challenges of this situation. However, there are no clear criteria and guidelines for the design, installation, and operation of these screening centers worldwide. In this study, a novel NCMSC (non-contact modular screening center) was developed that addresses the problems of existing screening centers and the risk of cross-infection in screening centers during the COVID-19 testing process. This facility aims to evaluate the effect of the cross-infection prevention of the viruses and ventilation performance for rapid virus discharge from indoor spaces.
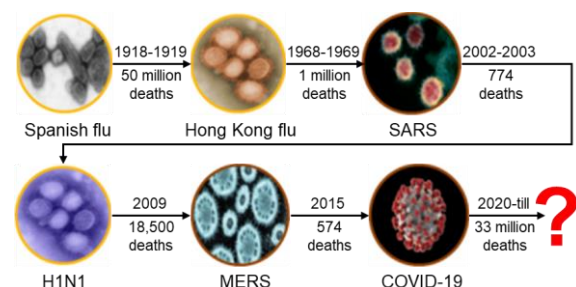

Fig. 1 - Brief outline of respiratory viral disease outbreaks.

2. Methodology

The initial step includes the classification of the different types of COVID-19 screening centers currently in operation and a novel NCMSC was proposed. The design optimizations of the space configuration and ventilation system are key factors in reducing the risk of cross-infection. The principal function of the ventilation strategy based on the NCMSC setup is to effectively block the movement of indoor aerosol that transmits the COVID-19 virus to other spaces and to discharge the viral particles quickly. The CFD (computational fluid dynamics) analysis of the ventilation system was performed using three design alternatives with different ventilation rates and balance of SA (supply air) and EA (exhaust air). The evaluation of the ventilation performance confirms the effect of the cross-infection prevention of the COVID-19 virus, which can be indirectly evaluated by analysis of airflow profiles of velocity and pressure differential in the rooms. And full-scale field measurements were performed under similar conditions as the numerical analysis to overcome the lack of experimental data on indoor airflow patterns. In addition, the results of the measurements were compared and verified using the results of the CFD simulation. The experiment was performed using PIV (particle image velocimetry), which can simulate virus particles.

3. Development of a NCMSC

A NCMSC was developed that uses biosafety cabinets and negative pressure booths to address the problems of existing screening centers and enable safe, fast, and convenient COVID-19 testing. NCMSC is a mobile modular building that can be quickly moved, installed, and operated in the required area depending on the COVID-19 testing demand. This type of medical modular facility can reduce the risk of cross-infection between rooms by achieving the airtightness performance of the structure. In particular, a non-contact automated system was applied to the entire testing process, from medical interviews and body temperature measurements to specimen transport, to prevent infection from the source. NCMSC increases the accessibility of patients to the screening center and provides adequate protection for HCWs.

NCMSC is a safe medical facility equipped with negative pressure zones, namely the AR (anteroom) and SCB (specimen collection booth), and positive pressure zones, such as the ER (examination room), as shown in Fig. 2. Moreover, it implemented two-stage negative pressure control to prevent virus

leakage. The air change rate was set to 12 ACH [5], [6] or above, which is the standard for an airborne infectious isolation room, and the pressure differential was set to maintain 25 Pa or above. Subsequently, the ER maintained positive pressure, and a low-noise fan and high-performance air filter (PM2.5 99.97%) were applied to prevent infection among HCWs.
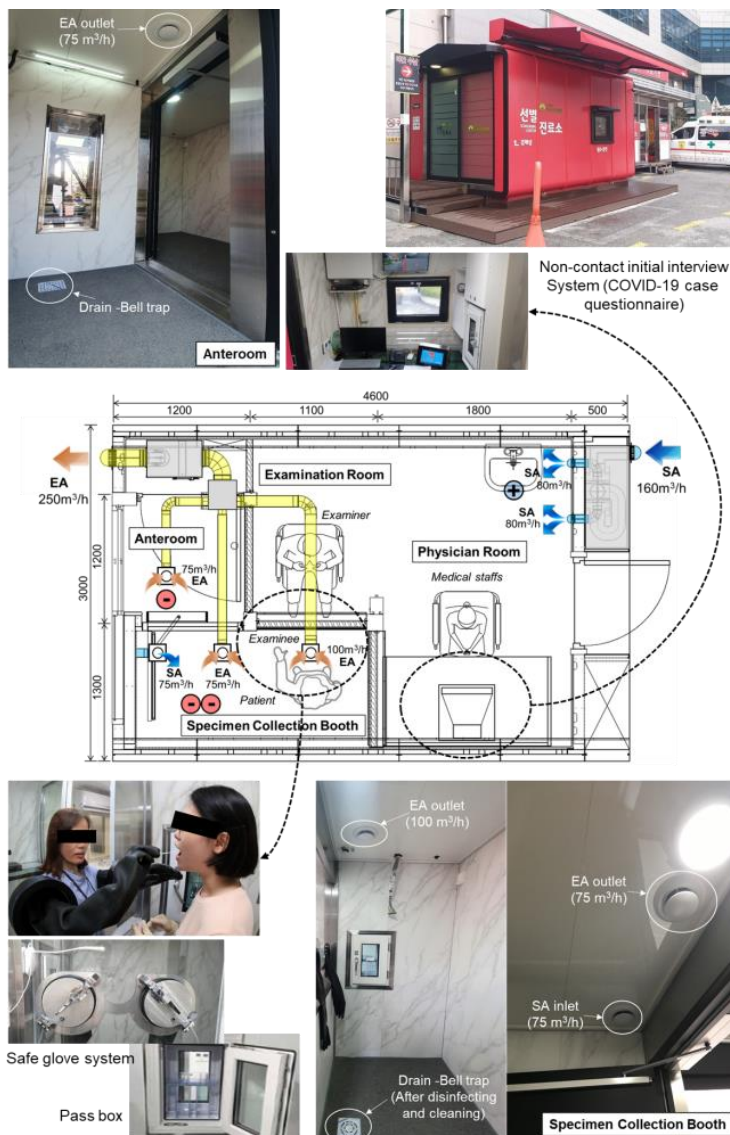

Fig. 2 - Layout of the NCMSC and location of SA/EA for the ventilation system.

This pressure differential is based in the case in which the door is closed and not when the door is opened or with the movement of people. The total air change rate was set to be 12-30 ACH for an effective discharge of viruses that can be produced in SCB. The screening center ventilation system provides a safe air environment for HCWs and individuals to be tested against infection. Therefore, the appropriate arrangement of the SA and EA outlets of the ventilation system is an important consideration for adequate indoor airflow. The ventilation system and pressure differential performance should be reviewed and the airtightness and the area of opening of the structure

should be optimized to maintain pressure differential through simulation analysis results and prevent aerosol viral diffusion and infection between rooms for SCB and ER in NCMSC. On the other hand, the indoor space needs to be comparted into zones, and the plan should be simplified when performing CFD analysis that can investigate the inter-zonal air movement from the SCB to the ER. In addition, three ventilation strategies and operating conditions were presented to evaluate the ventilation performance based on the SA and EA conditions of each room.

4. Numerical analysis

A quantitative analysis of the effect of the COVID-19 virus cross-infection prevention and a ventilation strategy to prevent the transmission are needed and should be established in the developed NCMSC. In this study, the airflow that can cause the diffusion of the COVID-19 virus was analyzed using STAR CCM+ CODE for CFD analysis of the NCMSC ventilation system. The effects of the airflow velocity and room pressure control based on the operation of the ventilation system on the viral transmission were investigated. The safe location of the ER, where HCWs were present, was also determined.
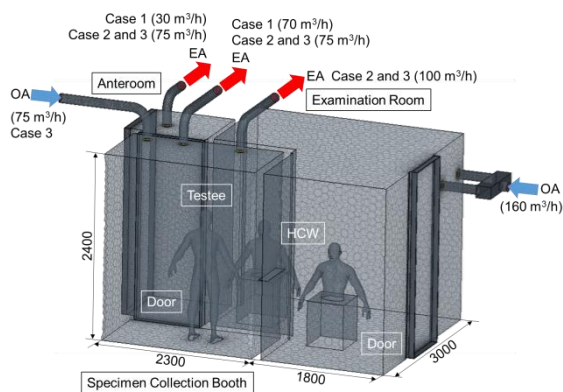
4.1 CFD modelling

Fig. 3 - NCMSC mesh of the CFD model.

The dimension of the CFD domain was 4100 × 3000 × 2400 mm (L × W × H). **Fig. 3** shows the division of SCB, AR, and ER. The EA outlet was located on the ceiling of the SCB and AR to avoid its effect on the airflow generated from the door, and the SA inlet was installed in the ER that required a positive pressure. Both SA and EA systems were applied in the SCB for effective ventilation. On the other hand, the SA flowrate of the ER and the two circular diffusers placed on the upper wall was set to 160 m³/h (6 ACH). An EA outlet was installed on the ceiling in AR. In particular, the airflow rate of EA was 30 m³/h (12 ACH) for Case 1, and 75 m³/h (30 ACH) for Cases 2 and 3. Meanwhile, an EA outlet was installed in the SCB with an EA flowrate of 75 m³/h (12 ACH) for Case 1. In addition, two EA outlets were installed for Cases 2 and 3 with an EA flowrate of 175 m³/h (30 ACH). Furthermore, Case 3 applied the SA system in which a circular diffuser was

installed on the ceiling with a flowrate of 75 m³/h. The negative pressure control was performed in SCB, and analyses were performed with all doors closed. The shortage of SA for EA was supplemented through door gaps of adjacent rooms, and the direction of airflow was from the ER to the SCB. Finally, a relief damper was installed to prevent backflow.

The mesh density was adjusted by dividing the analysis domain to consider the importance of the analysis domain. The total number of grid cells was 8,176,419. The analysis and convergence conditions were set to a residual range of 10^{-4}, and the turbulence analysis model was based on the standard k–ε model. The boundary conditions of the simulations are listed in **Tab. 1**.

Tab. 1 – CFD boundary conditions with airflow rates.

	Case 1 (Baseline)	Case 2	Case 3
Supply (ER)	160 m³/h	160 m³/h	160 m³/h
Transfer (ER to SCB)	25 m³/h	40 m³/h	30 m³/h
Supply (SCB)	N/A	N/A	75 m³/h
Exhaust (SCB)	70 m³/h	175 m³/h	175 m³/h
Exhaust (AR)	30 m³/h	75 m³/h	75 m³/h
Transfer (AR to SCB)	45 m³/h	135 m³/h	70 m³/h
Lying manikins	Uniform heat flux: 62 W, no slip boundary		
Walls	2 and 1 W/m² at ceiling/floor, no slip boundary		
Bedside	Adiabatic wall boundary condition		
Grid cells	8,176,419		
Turbulence model	Standard k–ε model		

4.2 Simulation results

In this study, the velocity of air supplied through the SA inlet and gap of the door, the velocity of air exhausted through the EA outlet, and the pressure differential between rooms were evaluated for the steady-state airflow in the rooms using the standard k–ε model. Then, the ventilation performance through which the virus is assumed to be an aerosol of SCB is predicted. **Tab. 2** lists the CFD analysis results for NCMSC that were derived for the three ventilation cases by combining different air change rates and SA/EA methods.

4.2.1 Airflow velocity

Fig. 4 shows the horizontal airflow velocity profile at a height of 1.5, and 2.2 m from the floor for each Case. The air change rates for AR and SCB in Case 1, which only applied the EA system, was set to 12 ACH. The velocity values were in the range of 0.0374 to 0.0506 m/s by examining the average airflow velocity distribution for each height of the SCB, indicating that the airflow progressed slowly and the air was gradually exhausted. The total airflow rate of EA, AR, and ER were 67.7, 24.2, and

43.5 m³/h, respectively. Specifically, in the case of AR, the air was exhausted at an air flowrate of 29.0 m³/h with a similar velocity of approximately 0.0365~0.0414 m/s with some of the air moved to the SCB.

Tab. 2 – CFD simulation results of the airflow profile; velocity and pressure differential.

Room	Velocity (m/s)	Case 1 (Baseline)	Case 2	Case 3
SCB	Z = 0.5m	0.0506	0.0945	0.1756
	Z = 1.5m	0.0442	0.0852	0.1781
	Z = 2.2m	0.0374	0.0861	0.1236
	Y = 0.5m	0.0743	0.1125	0.1201
	Y = 1.0m	0.0937	0.1095	0.1454
	X = 0.5m	0.0526	0.1150	0.1152
	Average	0.0587	0.1122	0.1786
AR	Z = 0.5m	0.0414	0.0977	0.1166
	Z = 1.5m	0.0365	0.0931	0.1086
	Z = 2.2m	0.0406	0.1003	0.1110
	X = 0.5m	0.0379	0.0857	0.1167
	Average	0.0410	0.0988	0.1166
ER	Z = 0.5m	0.1499	0.1469	0.1470
	Z = 1.5m	0.1412	0.1381	0.1405
	Z = 2.2m	0.2825	0.2591	0.2814
	Y = 0.5m	0.0748	0.0838	0.0755
	Y = 1.0m	0.0783	0.0826	0.0818
	Average	0.1652	0.1664	0.1638
Pressure differential (Pa)		Case 1 (Baseline)	Case 2	Case 3
SCB ↔ ER		-14.62	-18.17	-25.25
SCB ↔ AR		-1.39	-1.87	-3.02

On the other hand, the air change rates for AR and SCB in Case 2, which only applied the EA system were set to 30 ACH. The average air velocity profile for each height of the SCB was in the range of 0.0852 to 0.0945 m/s, indicating that the airflow velocity was increased twice than in Case 1, and the air was exhausted at an air flowrate of 169.2 m³/h. At this time, air was introduced from AR and ER at an air flowrate of 38.7 and 169.2 m³/h, respectively. The air in the AR is exhausted at an air flowrate of 72.5 m³/h with a velocity range of 0.0931 to 0.1003 m/s with some of the air moves to the SCB.

Furthermore, the air change rates for AR and SCB in Case 3, which applied both EA and SA systems in the SCB were set to 30 ACH. The average airflow velocity, SA airflow rate, and EA airflow rate were from 0.1236 to 0.1781 m/s, 72.5 m³/h, and 169.2 m³/h, respectively. The average airflow velocity profile for each height increased by approximately 1.7 times than in Case 2. At this time, air was introduced from AR and ER at an air flowrate of 29.0 and 67.6 m³/h, respectively. The air in AR was exhausted at an air flowrate of 72.5 m³/h with a velocity ranging from 0.1086 to 0.1166 m/s, and some of the air moves to the SCB.

4.2.2 Pressure differential

The pressure differential is another factor that can determine the effect of COVID-19 cross-infection prevention on NCMSC. A negative pressure should be maintained in the contaminated zone (SCB) and a positive pressure should be maintained in the clean zone (ER) to ensure that the aerosol COVID-19 viruses in SCB do not flow to the ER.

Fig. 5 shows the pressure differential profile for each height of 0.5 and 1.5 m from the floor for each case in which the key parameter is the pressure differential between SCB and ER. It is less likely that
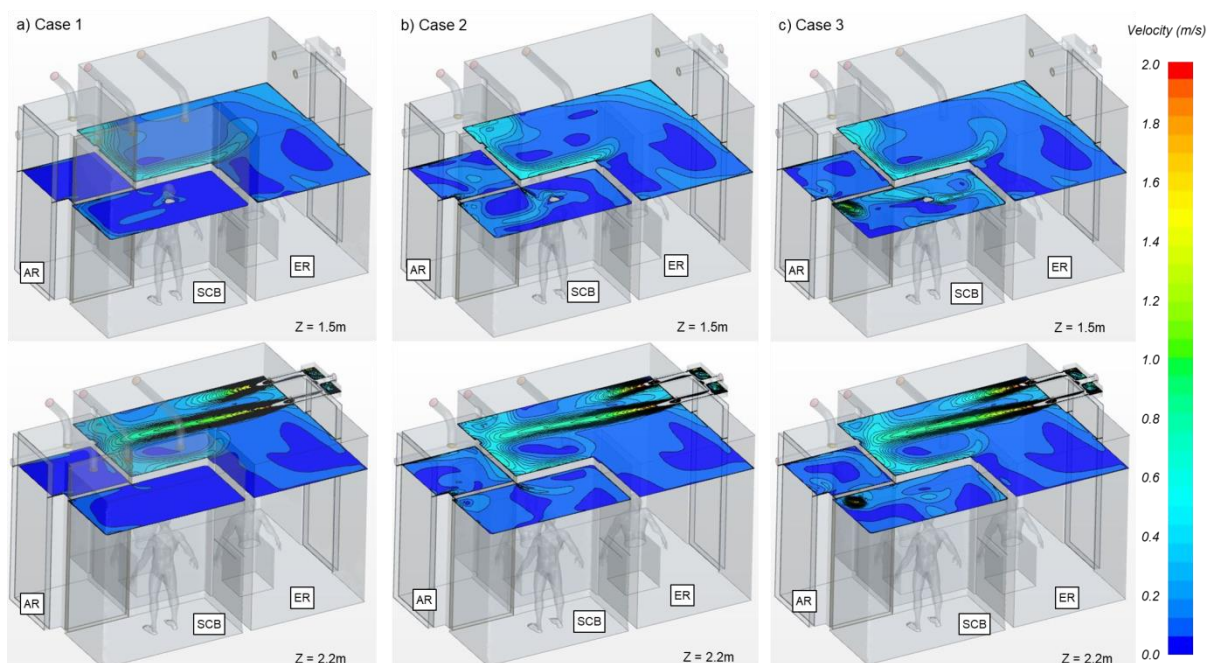

Fig. 4 - Velocity magnitude contours at the cross-sections (Z = 1.5m and 2.2m) in NCMSC for different ventilation conditions.

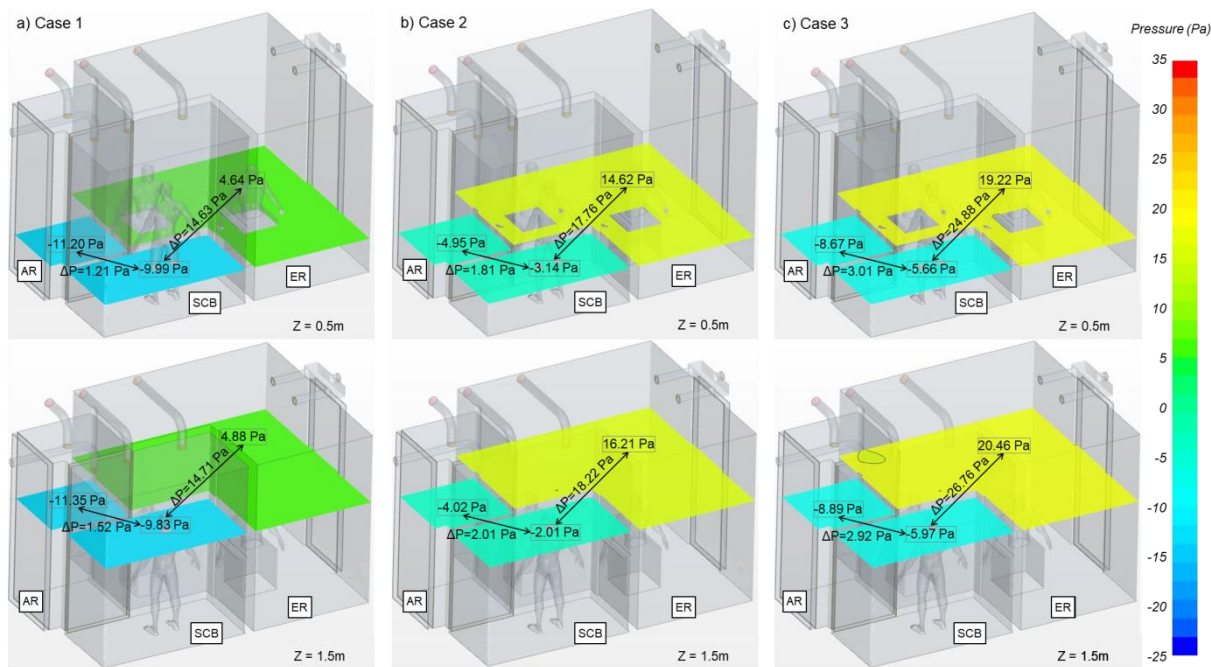**Fig. 5** - Pressure magnitude contours at the cross-sections (Z = 0.5m and 1.5m) in NCMSC for different ventilation conditions
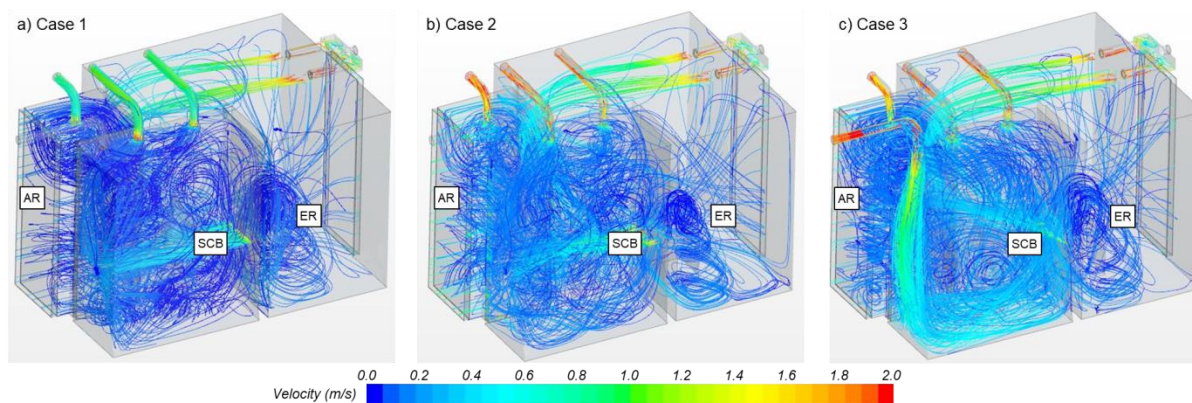

Fig. 6 - Streamline visualization of the velocity field in NCMSC for different ventilation conditions.

COVID-19 viruses migrate from SCB to the ER if the pressure is great between these two rooms. The average pressure differential for Cases 1, 2, and 3 were -14.62, -18.17, and -25.25 Pa, respectively. The analysis showed that the SCB was properly controlled for all cases to maintain the negative pressure. In addition, the effect of the cross-infection prevention of COVID-19 entering the ER is considerably enhanced because the pressure differential increases from Case 1 to Case 3. The pressure differential between the SCB and AR functions were also tested to prevent the cross-infection of other individuals to be tested waiting outside. The average pressure differential for Cases 1, 2, and 3 were -1.39, -1.87, and -3.02 Pa, respectively. Moreover, both SCB and AR maintain a negative pressure. However, the pressure differential values for Cases 1 and 2 are not within the appropriate range of the recommended pressure differential of at least -2.5 Pa based on the criteria applied to the airborne infectious isolation room [7]. Therefore, Case 3 was found to be the most effective method for preventing COVID-19 cross-infection.

4.2.3 Ventilation

Fig. 6 shows the airflow streamlines across the entire MCMSC space. It is apparent that for SCB, which applied both SA and EA systems in Case 3, the ventilation is active across the entire room compared to Cases 1 and 2, which only applied the EA system. The airflow velocity results of 0.0587 m/s for Case 1 and 0.112 m/s for Case 2 were obtained by examining the overall average airflow velocity of the room, indicating that the velocity of Case 2 increased by 1.9 times than Case 1. In addition, the airflow velocity was 0.1786 m/s for Case 3, indicating a velocity increase of 1.6 times than Case 2 and 3.0 times than Case 1. It is expected that Case 3 will enhance the ventilation performance and facilitate an effective discharge of the aerosol COVID-19 viruses.

5. Experimental analysis

This experimental study analyzes the airflow pattern based on the application of both SA and EA systems to facilitate ventilation in SCBs. The airflow patterns based on the CFD analysis may be different depending on the placement of the SA inlet and EA outlet and open-closed status of the door. Full-scale field measurements were performed under similar conditions used in the numerical analysis. PIV (particle image velocimetry) was used to conduct experiments for airflow behavior characterization and examination of the leakage area through visualization of particles simulating viruses in SCB and to verify the safety of the developed NCMSC against cross-infection. PIV is a non-intrusive measurement method that allows the application of all optical approaches to airflow by adjusting various parameter constraints, including image and recording characteristics, laser sheet properties, and analysis algorithms [8].
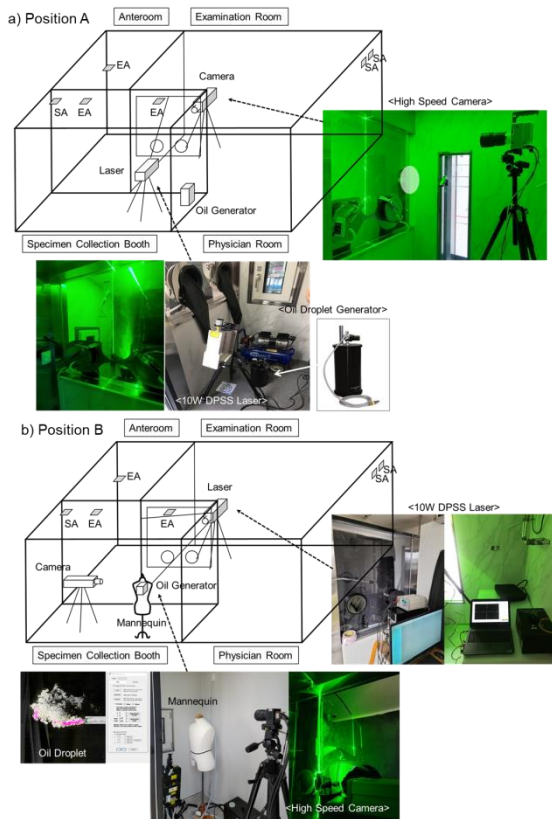

Fig. 7 - Experimental set-up for the PIV.

5.1. Experimental set-up

The purpose of the experimental study was to obtain information on airflow patterns between the SCB and ER. Fig. 7 shows the experimental setup and perspective view of the PIV set-up. Two-dimensional flow fields were measured at different positions of the camera and laser. First, the camera was installed in the ER, and the laser and oil droplet generator were installed in the SCB. The overall airflow in the rooms adjacent to the tested individual was observed at Position A. Moreover, at Position B, the laser was installed at the ER and the camera. Then, at the same position, the oil droplet generator was installed in the SCB to ensure that the droplet came out from the mouth of the manikin, a simulation model of the individual to be tested. Subsequently, the exhaust airflow was observed.

Four different PIV measurements were performed for four different combinations, as shown in Tab. 3. First, the PIV measurement was performed at Position A for Case 2, where only the EA system was applied, and Case 3, where both EA and SA systems were simultaneously applied in the ventilation system of the SCB, that were analyzed in the CFD simulation. Subsequently, the experimental setup was changed and the ventilation performance at Position B was examined with the door between the AR and SCB closed and open for Case 3. In principle, all doors are closed during the COVID-19 testing. However, the doors were opened and ventilation was performed before the next individual to be tested entered the SCB after each examination. Therefore, the ventilation effect in this situation was investigated.

Tab. 3 - Measuring cases with the PIV equipment.

Measurement	Cases	Position	Door between SCB and AR
PIV A1	Case 2	A	Closed
PIV A2	Case 3	A	Closed
PIV B1	Case 3	B	Closed
PIV B2	Case 3	B	Open

5.2. Measurement results

In Case 2, the PIV experiment was conducted only with the EA system applied in SCB, while both SA and EA systems were used in Case 3. The pressure differentials of SCB and ER with the ventilation system turned on are ΔP = -21.8 and -29.3 Pa, respectively. The negative pressure in the SCB was properly maintained for both cases (Cases 2 and 3). Tab. 4 lists the time-averaged airflow velocity profiles in the SCB. The experimental results were divided into two parts based on the location of the PIV measurements.

Tab. 4 – PIV measurement results of airflow velocity.

Measurement	Cases	Velocity (m/s)		
		Mean	Min	Max
PIV A1	Case 2	0.0098	0.0031	0.0607
PIV A2	Case 3	0.0541	0.0120	0.2531
PIV B1	Case 3	0.0536	0.0238	0.1124
PIV B2	Case 3	0.1042	0.0117	0.1747

Moreover, Fig. 8 shows the experimental results for the vertical airflow velocity. The velocity vector consists of two time-averaged velocity components V_x(m/s) and V_y(m/s) along the X- and Y-axes, respectively. All the results presented are based on the map of the average velocity vectors. Fig. 8a) shows the average velocity of Case 2 for Position A

(i.e., PIV A1). The particle movement velocity in the SCB was found to be very slow with almost no airflow for a maximum airflow velocity of 0.0607 m/s and an average airflow velocity of 0.0098 m/s. The air exhaust efficiency is lowered because the air flowing in from the AR is not sufficient due to the high airtightness of the structure. On the other hand, the average airflow velocity of PIV A2 in Case 3 shown in **Fig. 8b)**, where SA and EA systems were applied to the SCB, was 0.0541 m/s, indicating a four-time increase than PIV A1. In addition, the generated particles were smoothly discharged through the upper EA outlet. The make-up air was smoothly supplied to improve the exhaust efficiency. In addition, the result after the examination of the leakage area showed that there were no particles generated inside the SCB that escaped through the gap in the wall in contact with the ER. Therefore, the cross-infection by viruses is not expected to occur since there was no airflow from the contaminated zone (SCB) to the clean zone (ER) in PIV A1 and PIV A2.

Fig. 8c) shows the average velocity of Case 3 for Position B (i.e., PIV B1). The maximum airflow velocity of PIV B1 was 0.1124 m/s and the average airflow velocity was 0.0536 m/s, indicating that the average velocity of the particles generated in the SCB is the same as that in PIV A1. This result is expected because they were both performed under the same conditions except for the measurement position Finally, **Fig. 8d)** shows the average velocity of Case 3 for Position B (PIV B2). The same condition was applied to PIV B2 as PIV B1, but the door to the AR was opened. In this case, the results showed that the maximum airflow velocity was 0.1747 m/s, the average airflow velocity was 0.1042 m/s, and the velocity of the generated particles increased more than twice than that of PIV B1, confirming the improvement in the ventilation performance. However, it is a principle to close the door during specimen collection to prevent airflow in adjacent rooms. Therefore, it is recommended to operate the ventilation system with the door open before the next individual to be tested enters to increase the cleaning and disinfection effect after collecting the specimen.
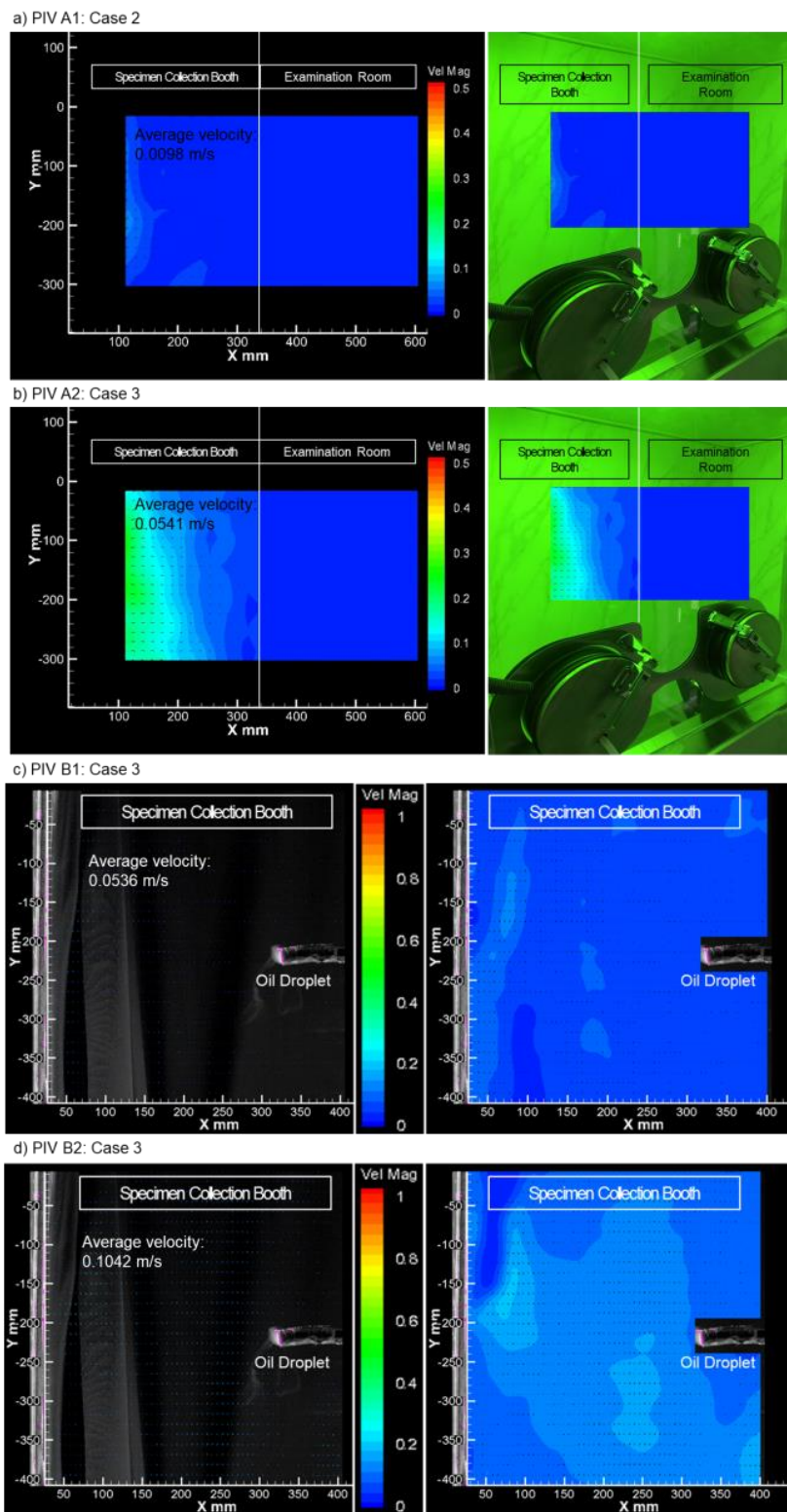

Fig. 8 - Time-averaged air distribution under PIV cases.

6. Conclusion

A novel non-contact modular screening center (NCMSC) was developed to address the potential risk of cross-infection in screening centers during COVID-19 testing. The main aim of this study was to evaluate the effects of virus cross-infection prevention and ventilation performance on rapid virus discharge based on an actual project and to

employ both numerical analysis and experimental measurements. The main findings of this study are as follows.

(1) In the proposed NCMSC, the space configuration that enables non-contact specimen sampling between HCWs and tested individuals were implemented, and the pressure differential control such as maintaining negative-positive pressure were reflected. In addition, the proposed SCB design allows sufficient ventilation for safe use by the next patient to be tested.

(2) Furthermore, design optimization was performed using three alternatives by combining different air change rates in each room and applying the SA/EA system for the ventilation strategy of NCMSC to prevent the transmission of the COVID-19 virus.

(3) The results of the CFD analysis showed that the effect of cross-infection prevention was the most significant in Case 3 in the SCB, where the negative pressure must be maintained, at the ventilation rate of 30 ACH and a pressure differential of -25 Pa or more between ER using both SA and EA systems. Compared to Case 2, in which only the EA system was applied under similar ventilation rate conditions, the airflow velocity in the room increased by approximately 0.6 times. Moreover, compared to Case 1, in which only the EA system was applied with a ventilation rate of 12 ACH, the airflow velocity increased by more than two times. This demonstrated the improvement of the ventilation performance in Case 3.

(4) The result of the PIV experiments in Case 3 shows that the pressure differential between an ER of -30 Pa or more was maintained, and the effect of cross-infection prevention was excellent compared to -22 Pa in Case 2, and the ventilation performance with an increase in airflow velocity by four times was also achieved.

Based on the results of this study, the standards for the installation and operation of the COVID-19 screening centers are proposed. It is necessary to implement space configuration and secure airtight performance to ensure that all tests can be performed using non-contact methods. To maintain the negative pressure of SCB and prevent cross-infection between HCWs and individuals to be tested, a ventilation rate of 30 ACH, and a pressure differential of -15 Pa or higher is recommended. In addition, a simultaneous application of both SA and EA systems is effective in facilitating a smooth discharge of the airborne COVID-19 virus.

7. Acknowledgement

8. References

[1] Lim, T., Cho, J., Kim, B.S. The predictions of infection risk of indoor airborne transmission of diseases in high-rise hospitals: Tracer gas simulation. Energy Build. 2010;42(8):1172-1181.

[2] Noor, R., Maniha, S.M. A brief outline of respiratory viral disease outbreaks: 1889-till date on the public health perspectives. Virusdisease. 2020;31(4): 441-449.

[3] Asad, H., Johnston, C., Blyth, I. Holborow, A., Bone, A., Porter, L., Tidswell, P., Healy, B. Health Care Workers and Patients as Trojan horses: a COVID19 ward outbreak. Infect Prev Pract. 2020;2(3):100073.

[4] Hassan, A.M., Megahed, N.A. COVID-19 and urban spaces: A new integrated CFD approach for public health opportunities. Build. Environ. 2021;204:108131.

[5] CDC, Guidelines for preventing the transmission of mycobacterium tuberculosis in health-care facilities. US Department of Health and Human Services, Public Health Services, Federal Register. 1994.

[6] Cho, J., Woo, K., Kim, B.S. Removal of airborne contamination in airborne infectious isolation rooms. ASHRAE J. 2019;61(2):8-21.

[7] Cho, J. Investigation on the contaminant distribution with improved ventilation system in hospital isolation rooms: Effect of supply and exhaust air diffuser configurations. Appl. Therm. Eng. 2019: 148:208-218.

[8] Cao, X., Liu, J., Jiang, N., Chen, Q. Particle image velocimetry measurement of indoor airflow field: A review of the technologies and applications. Energy Build. 2014;69:367-380.